Nonlin. Processes Geophys. Discuss., doi:10.5194/npg-2016-13, 2016
Manuscript under review for journal Nonlin. Processes Geophys.
Published: 27 January 2016

Nonlinear Processes in Geophysics
Discussions
Open Access
EGU

Extended Application of the CNOP-P method in the Inner Mongolia using the Common Land Model

Bo Wang[a,b,d], Zhenhua Huo[c,d], Yujing Yuan[e], Shang Wu[b]

[a] Institute of Applied Mathematics, Henan University, 475004 Kaifeng, China

[b] School of Mathematics and Statistics, Henan University, 475004 Kaifeng, China

[c] University of Chinese Academy of Sciences, 100049, Beijing, China

[d] LASG, Institute of Atmospheric Physics, Chinese Academy of Sciences, 100029, Beijing, China

[e] School of Mathematics, Shandong University, 250100 Jinan, China

Correspondence to: Bo Wang (wangbo_sdu@163.com)

Nonlin. Processes Geophys. Discuss., doi:10.5194/npg-2016-13, 2016
Manuscript under review for journal Nonlin. Processes Geophys.
Published: 27 January 2016

Nonlinear Processes in Geophysics
Discussions
Open Access
EGU

Abstract: An extension method of the conditional nonlinear optimal perturbation about parameter (CNOP-P) is adopted to study the soil parameter optimization for the Hulunbeier Steppe within the common land model (CoLM) with the differential evolution (DE) method. Using National Center for Environmental Prediction/Department of Energy (NCEP/DOE) Atmospheric Model Intercomparison Project-Ⅱ (AMIP-Ⅱ) 6-hourly Reanalysis Gaussian Grid data and National Meteorological Center (NMC) Reanalysis 6-hourly surface fluxes data, three experiments (Ⅰ and Ⅱ) were designed to study the impact of the percentages of sand and clay of the shallow soil in CoLM on simulating the shallow soil moisture. To study the shallow soil moisture and the latent heat flux simultaneously, experiment (Ⅲ) is designed. The optimal parameters obtained by the extended CNOP-P method are used to predict the shallow soil moisture in the following month. In all the three experiments, after optimization stage, the optimal soil parameters could significantly improve the simulation ability of CoLM in the Inner Mongolia to the shallow soil moisture at the stage of prediction; the optimal parameters attained by the double-parameter optimal experiment could make CoLM simulate the shallow soil moisture better than the single-parameter optimal experiment in the optimization slot. Moreover, the results of experiments (Ⅰ and Ⅱ) justify the conclusion that the more accurate the atmospheric forcing data and observation data are, the more effective the results of optimization will be.

Keywords: CNOP-P, parameter optimization, shallow soil moisture, CoLM, Inner Mongolia

1. Introduction

With the population explosion, the atmospheric environment pollution, the marine ecological deterioration, the land erosion and desertification, the sharp drop in fores resources, the acid harm, the extinction of species, the water pollution and the toxic waste pollution, global warming has recently been a serious problem that more and more scientists are concerned with. Global worming will result in the global climate

Nonlin. Processes Geophys. Discuss., doi:10.5194/npg-2016-13, 2016
Manuscript under review for journal Nonlin. Processes Geophys.
Published: 27 January 2016

change including glacial ablation, sea level rise, floods, landslides, debris flow and so on. In addition, with global warming, the atmospheric temperature increases and the evaporation increases, so there is a severer trial in the areas which usually lack of rain with arid climate, the semi-arid areas which were not covered with plants well may be degenerated into the semi-desert areas, and so global warming may induce the acceleration of the desertification in the inland areas.

China is one of the countries which are severely affected by desertification. Desertification in Northern China has been an important problem which needs to be solved urgently for national economic and social development, with the wide distribution and rapid development of the desertification. In China, Inner Mongolia Autonomous Region is the most serious region affected by the desertification , and in recent years, there are great temperature and precipitation changes(Su et al., 2008; Han et al., 2010; Zhang et al., 2014), which can influence the climate of Inner Mongolia. So, it is necessary to predict accurately the variables, such as temperature, precipitation, soil moisture and latent heat et al., which are very important to study the drought degree of Inner Mongolia Autonomous Region so that it could supply some help for the management and control of desertification, especially for the agricultural and animal husbandry production.

Hulunbeier Steppe is located in the northeast grassland of China's Inner Mongolia Autonomous Region, west of the Greater Khingan Mountains. The Greater Khingan Mountains separates the Hulunbuir Steppe into two kinds of climate. The eastern ridge is the monsoon climate and the western ridge is the continental climate from the point of the climate types. From the point of the annual precipitation types, the eastern ridge is the semi-humid climate and the western ridge is a semi-arid climate. The special geographical position of Hulunbuir brings about that the total characteristics in climate of Hulunbiur Steppe is cold and dry in winter, hot and rainy in summer and the annual and daily temperature differences are large. Since 1999, the climate of Hulunbiur became unusual: the annual precipitation is low, the spring is droughty and windy, the summer continues the high temperature, water evaporation capacity increases and the level of drought increases. Located in the arid and semi-arid area of

Nonlin. Processes Geophys. Discuss., doi:10.5194/npg-2016-13, 2016
Manuscript under review for journal Nonlin. Processes Geophys.
Published: 27 January 2016

North China, the Hulunbiur Steppe is one of the important livestock husbandry bases and high quality natural pastures in China, so, it is extremely important to study the land surface of the Hulunbiur Steppe.

The land surface processes mainly study all the processes which are closely related to the atmosphere movement at the underlying surface. They contain the complex soil water heat transmission and vegetation physiological and biochemical processes. They are one of the fundamental biochemical and physical processes which could affect atmospheric circulation and climatic change. In order to understand the land surface processes better, it is worth improving the land surface models (LSMs). Sun (2005) pointed out that the parameter values in some physical processes are inaccurate, and the simulations of LSMs are also inaccurate with the impact of inaccurate parameter values. So, it is meaningful to optimize the parameters of LSMs. Some researchers have investigated the parameter optimization in LSMs. With the Chameleon Surface Model (CHASM), Xia et al. (2002, 2004a, 2004b) studied the adaptability of different parameter optimization methods in LSMs. Their results show that the parameter optimization in LSMs could improve LSMs in some respects. Bastidas et al. (2006) adopted the multicriteria method to optimize the parameters in four different LSMs at five stations. Their researches indicate that the parameter optimization can improve LSMs. Li et al. (2011a, 2011b) optimized parameters in a LSM with the expanded CNOP method and their work show that the expanded CNOP method can improve the simulation ability of the LSM. So, with a suitable method, the parameter optimization of LSMs could be carried out effectively. There are several parameter optimization methods suitable to LSMs like the Shuffled Complex Evolution (SCE-UA) method, the Multistep Auromatic Calibration Scheme (MACS), the Multi-Objective Complex Evolution (MOCOM-UA) method and the difference evolution (DE) method. All the prior three methods use a complex method named the complex evolution method, need massive computation, require tedious programming and have poor transferability. DE method has a rapid computability, a strong transferability and a simple designed structure. So, DE method is suitable to execute the parameter optimization of LSMs.

Nonlin. Processes Geophys. Discuss., doi:10.5194/npg-2016-13, 2016
Manuscript under review for journal Nonlin. Processes Geophys.
Published: 27 January 2016

Soil moisture is important to many hydrological, biogeochemical and biological processes. It plays a key role in processes of the complex soil water heat transmission and vegetation physiological and biochemical, and also has a direct impact on the soil properties, field climate and the decomposition of nutrients. In addition, soil moisture is one of the important conditions for the movement of the microbes in the soil and the breeding of crops. It is affected seriously by the soil property, the atmosphere, the vegetation and so on. If the soil moisture is too high, it is easy to worsen the soil aeration, affect the life action of crops such as the growth and the respiration of the root of crops and the activity of the microbes in the soil. Thereafter, soil moisture can affect plowing and sowing a field, as well as the soil temperature. For government agencies and private companies, who are concerned with weather and climate, geotechnical engineering, flood control, water quality, soil erosion, slope failure, and so on, information about soil moisture is very essential. So the investigation of the ability of land surface models to simulate shallow soil moisture is very important in the aspect of the improvement of environment, the development of the agriculture and the control of desertification.

The conditional nonlinear optimal perturbation (CNOP) method is put forward and developed by Mu et al. (2003, 2010) respectively. The approach of conditional nonlinear optimal perturbation related to parameter (CNOP-P) is used to attain the optimal parameter perturbation, whose nonlinear evolution in the forecast stage gains the optimal value and it is one special case of CNOP. CNOP method has been employed to investigate the response of a grassland ecosystem to climate change and human activities (Mu and Wang, 2007; Sun and Mu, 2011), ENSO predictability (Mu and Duan, 2003; Duan et al., 2004; Duan and Mu, 2006, 2009; Duan et al., 2008; Duan et al., 2009a, 2009b; Duan and Luo, 2010; Duan and Zhang, 2010; Mu et al., 2010), the sensitivity analysis to the eutrophication of lakes (Wang et al., 2012) and so on, and a series of research results are achieved. Sun and Mu (2013, 2014) used the CNOP-P method to study the maximal variation in estimating the net primary production (NPP). The results show that CNOP-P method can capture the characteristic of nonlinear dynamical system As CNOP-P could make the dynamic

Nonlin. Processes Geophys. Discuss., doi:10.5194/npg-2016-13, 2016
Manuscript under review for journal Nonlin. Processes Geophys.
Published: 27 January 2016

system have the largest nonlinear development in the forecast stage, and it regards both the sensitivity of the objective parameter to the dynamic system and the influence of the nonlinearity of the dynamic system to the evolution from the initial moment to the forecast stage, CNOP-P method could possibly be extended and then applied to the area of parameter optimization in LSMs. Wang and Huo (2013) used the extended CNOP-P method and DE method to optimal some parameters in CoLM, and the results showed that after optimization, the simulation ability of CoLM can be improved to some degree in the North China Plain. So the expanded CNOP-P method and DE method are suitable to be employed to optimize the parameters in CoLM. So, it is reasonable to optimize the parameters with the expanded CNOP-P method and DE method to improve the simulating ability of soil moisture in the CoLM in the Hulunbiur Steppe.

As a state-of-the-art land surface model, Common Land Model (CoLM) is developed by Dai et al. (2001). This model combines the best features of three other land surface models, such as the Land Surface Model of Bonan (1996), the Biosphere-Atmosphere Transfer Scheme (BATS) of Dickinson et al. (1993) and the 1994 version of theChinese Academy of Sciences Institute of Atmo-spheric Physics LSM (IAP94) (Dai and Zeng, 1997). Luo et al. (2008), Xin et al. (2006) , Song et al. (2009a, 2009b), Zheng et al. (2009), Meng and Cui (2007) simulate China areas with CoLM, their results indicate that CoLM could simulate China well. So, in this paper, CoLM is employed to investigate the simulation of soil moisture in the Hulunbiur Steppe.

The percentage of sand and the percentage of clay in soil are important to the soil structure and they are different in different kinds of soil. Soil texture, which is related to the crop production and the field management, is an important soil characteristic and it is determined by the content of sand, clay and silt in the soil. Soil moisture could infect the proportion that water drains through the soil, water holding capacity, soil tilth, organic matter content, and drainage largely. As clayey soil has a larger water holding capacity than sandy soil, water could move more freely through the sandy soil than the clayey soil. Furthermore, in CoLM, the thermal conductivity of

Nonlin. Processes Geophys. Discuss., doi:10.5194/npg-2016-13, 2016
Manuscript under review for journal Nonlin. Processes Geophys.
Published: 27 January 2016

soil solid, the saturated matrix potential, the specific heat capacity of soil solid, the saturated hydraulic conductivity, and the porosity are produced according to the percentage of sand and the percentage of clay in soil. Therefore, we chose the percentage of sand and the percentage of clay as the optimal parameters in CoLM in this paper.

Actually, we have adopted the expanded CNOP-P method to study the impact of sand and clay in North China Plain (Wang and Huo, 2013). The results show that the expanded CNOP-P method and DE method are efficient to optimize the parameters sand and clay, and the parameters after optimization could make CoLM simulates the shallow soil moisture better in this area. In addition, we get the conclusion that the optimization results are affected by the atmospheric forcing data and the observations of the shallow soil moisture, and the more accurate the data are, the more significant the optimization results may be. In the purpose of investigating the impact of the percentage of sand and clay in the soil on the soil moisture in CoLM in Hulunbiur Steppe, a special arid and semiarid area, and comparing with the results of our former research, the same three experiments (I-III) as Wang and Huo (2013) are designed. In this paper, we will check this suspect with these three experiments.

2. The extension of CNOP-P

2.1 Definition of CNOP-P

In works of Mu et al. (2003, 2010), CNOP method is put forward and developed. CNOP-P is aimed at the parameter perturbation and it is one special case of CNOP. Here, we introduce this approach for reader's convenience. Let a nonlinear dynamic system be described as following equations:

$$\begin{cases} \dfrac{\partial w}{\partial t} = M\left(w, P\right), x \in \Omega, t \in [0, T] \\ w\left|_{t=0} = w_0 \right. \end{cases} \tag{1}$$

where $w(x,t) = (w_1(x,t), w_2(x,t), \cdots, w_m(x,t))$ is a model-state vector, M is a nonlinear partial differential operator, $\Omega \in \mathbb{R}^n$, $x = (x_1, x_2, \cdots, x_n)$, $0 < T < \infty$, w_0 is the initial value, $P = (P_1, P_2, \cdots, P_l)$ is a parameter vector and $\forall i = 1, 2, \cdots, l$, P_i is a model parameter invariant with time t.

Nonlin. Processes Geophys. Discuss., doi:10.5194/npg-2016-13, 2016
Manuscript under review for journal Nonlin. Processes Geophys.
Published: 27 January 2016

Suppose that $w(\tau)$ is the solution of Eq. (1) at time τ and M_τ is the nonlinear evolution operator from time 0 to time τ corresponding to the operator M, then the following equation will be established:

$$w(\tau) = M_\tau(w_0, P). \quad (2)$$

If $W(T;P)$ is the solution of Eq. (1) at time T corresponding to the parameter vector P and the initial value w_0, and $W(T;P)+w(T;p)$ is the solution of Eq. (1) at time T corresponding to the initial value w_0 and the parameter vector $P+p$, then the following relations will be established:

$$W(T;P) = M_T(w_0, P), \quad (3)$$

$$W(T;P) + w(T;p) = M_T(w_0, P+p), \quad (4)$$

where P is a parameter perturbation vector and $w(T;p)$ could indicate the departure level of the solution of Eq. (1) at time T with the basic state $W(T;P)$, which is caused by the parameter perturbation vector p.

We choose an appropriate norm $\|\cdot\|$ based on the detail physical background. The objective function under the given constraint condition $\|p\| \le \delta(\delta > 0)$ is defined as the following relation:

$$J(p) = G(w(T;p)), \quad (5)$$

where function $G(\cdot)$ evaluates the departure level which has been described in the previous paragraph. The parameter perturbation vector p' is the conditional nonlinear optimal parameter perturbation (CNOP-P), if and only if the parameter perturbation vector p' satisfies the following relation:

$$J(p') = \max_{\|p\| \le \delta} J(p). \quad (6)$$

So CNOP-P is the parameter perturbation vector which could make the objective function under the given constraint condition attain the maximum, i.e. it is the parameter perturbation vector that could cause the largest departure level of the dynamic system at time T.

2.2 Extension of CNOP-P

Nonlin. Processes Geophys. Discuss., doi:10.5194/npg-2016-13, 2016
Manuscript under review for journal Nonlin. Processes Geophys.
Published: 27 January 2016

In this paper, we use the extension of CNOP-P method proposed by Li et al. (2011a, b) to optimize the parameter of CoLM. Detailed introduction about the extension of CNOP-P can also be found in the work of Wang and Huo (2013). Here, we also give a simple introduction about it.

The parameter perturbation vector p' is considered as the extended CNOP-P if and only if:

$$J(p') = \max_{P+p \in \omega} J(p), \tag{7}$$

where P means the original parameter vector, p is the parameter perturbation vector, ω refers to the value range of the parameter vector and $J(p)$ means the objective function about p with the following form:

$$J(p) = -G(M_{0\to T}(w_0, P+p) - O), \tag{8}$$

where $0 \to T$ refers to the time period from time 0 to time T, $M_{0\to T}(w_0, P+p)$ is the simulations from time 0 to time T, O is the model state observation vector from time 0 to time T and the function $G(\cdot)$ evaluates the departure degree between the simulations and the observations from time 0 to time T.

Therefore, the extended CNOP-P is the parameter perturbation vector satisfying the constraint condition that could make the simulations closest to the observations. The method to get the extended CNOP-P is called the extension of CNOP-P method and it could be employed to conduct the parameter optimization of the land surface model.

3. The optimization method adopted to calculate CNOP-P

CoLM is a complex model, and the calculation of CNOP-P with the nonlinear optimization method depending on the adjoint method would need a lot of computational resource. It is against the standard that we should employ the optimization method with a little calculation cost. So we use the differential evolution method (DE method) as the optimization method in our experiments.

In 1995, Storn and Price (1995) proposed DE method to solve the Chebyshev Polynomial fitting Problem firstly. Liu et al. (2007) found that DE method is effective to solve the complex optimization problems. DE method is a parallel, random and

Nonlin. Processes Geophys. Discuss., doi:10.5194/npg-2016-13, 2016
Manuscript under review for journal Nonlin. Processes Geophys.
Published: 27 January 2016

global direct-search algorithm based on the population evolution with the character of sharing information in populations and remembering group optimal solutions. As a novel direct search method, DE method use a greedy genetic algorithm to maintain the excellent population member based on the real number encoding with excellent convergence properties. Given the randomly generated initial population, DE method solves the optimization on the basis of the theory of survival of the fittest, in accordance with the fitness value of every population. It has been applied and developed by many scholars to solve different problems (He and Wang, 2008; Yu et al., 2009). Sun and Mu (2009) have found that DE method is effective to obtain CNOP. Wang and Huo (2013) have used this method to calculate the extension of CNOP-P effectively. Their work show that it is effective to employ DE method to handle nonlinear and non-differentiable cost functions if the gradient of the cost function is hard to obtain or even not obtained. As the cost function about the parameters may become non-differentiable with the adjustment of the parameter, it is applicable to optimize the parameters in LSMs with DE method.

4. Experimental design and the numerical results

In this paper, NCEP/DOE AMIP-Ⅱ 6-hourly Reanalysis Gaussian Grid data and NMC Reanalysis 6-hourly surface fluxes data at NCEP/NCAR Center at the Hulunbiur Steppe $(48.5705^{\circ}N, 120^{\circ}E)$ are used. NMC Reanalysis 6-hourly surface fluxes data, which is currently kept using near real-time observations, is one product of NCEP/NCAR Reanalysis Ⅰ, which is the first of its kind of National Oceanic and Atmospheric Administration (NOAA). NCEP/DOE AMIP-Ⅱ 6-hourly surface fluxes data is one product of NCEP/DOE Reanalysis Ⅱ, which is the second version of NCEP/NCAR Reanalysis Ⅰ and starts from the beginning of the major satellite era with a better version of the model used, more observations added and assimilation errors corrected. Both NCEP/DOE AMIP-Ⅱ 6-hourly Reanalysis Gaussian Grid data and NMC Reanalysis 6-hourly surface fluxes data are used to investigate the simulation ability of CoLM to the shallow soil moisture. For convenience, we will call

Nonlin. Processes Geophys. Discuss., doi:10.5194/npg-2016-13, 2016
Manuscript under review for journal Nonlin. Processes Geophys.
Published: 27 January 2016

NCEP/DOE AMIP-Ⅱ 6-hourly Reanalysis Gaussian Grid data dataset Ⅰ and NMC Reanalysis 6-hourly surface fluxes data dataset Ⅱ in the following part of this paper. Dataset Ⅰ are the revise of dataset Ⅱ and they are more accurate than dataset Ⅱ. We will similarly call the percentage of sand in soil sand and the percentage of clay in soil clay. For the sake of investigating the impact of sand and clay on the shallow soil moisture, we designed two experiments (Ⅰ and Ⅱ), and simulated the shallow soil moisture in the following one month with the optimal parameters, which are gained in the duration of optimization. We select the root mean square deviation as the objective function with following form:

$$f_r = \sqrt{\frac{\sum_{i=1}^{n}(s_i - o_i)^2}{n}}, \tag{9}$$

where f_r refers to the root mean square deviation, n means the integral time steps, s_i represents the simulation value and o_i is the observation value at time i.

4.1 Experiment Ⅰ and the results

4.1.1 Experiment Ⅰ

The forcing data in dataset Ⅰ, which contain the precipitation and the large-scale precipitation, the specific humidity and the air temperature at 10 m above the ground, the wind component in northward direction and eastward direction at 10 m above the ground, the atmospheric pressure, the atmospheric longwave radiation and the incident solar radiation at surface, are used in CoLM in experiment Ⅰ. Here, we took the forcing data in dataset Ⅰ as the observation data, and compared the data in dataset Ⅰ with the simulation data of CoLM at the same time.

Generally speaking, CoLM might simulate the shallow soil moisture better after the double-parameter optimal experiment about sand and clay simultaneously than the single-parameter optimal experiment about sand or clay. So, we carried out both the single-parameter optimal experiment related to sand and clay separately and the double-parameter optimal experiment related to sand and clay simultaneously in this experiment. Through this experiment, we could check whether the optimal results are correct in the optimization slot at first, and verify whether the optimal parameters,

Nonlin. Processes Geophys. Discuss., doi:10.5194/npg-2016-13, 2016
Manuscript under review for journal Nonlin. Processes Geophys.
Published: 27 January 2016

which are obtained in the optimization slot, could make CoLM simulate the shallow soil moisture better at the stage of prediction, and whether the optimal parameters, which are attained in the double-parameter optimal experiment at the stage of optimization, could make the simulation ability of CoLM to the shallow soil moisture the best in the prediction slot. Notice that sand and clay (units: %) are independent inputs in CoLM, and both in the single-parameter experiment and the double-parameter experiment, these parameters should satisfy the constraint condition:

$0 \le \text{sand+clay} \le 100$, $0 \le \text{sand} \le 100$, $0 \le \text{clay} \le 100$.

4.1.2 The numerical results of experiment Ⅰ

Through a large number of numerical experiments during many different time ranges, the numerical results show that the optimal parameters could make CoLM simulate the shallow soil moisture more accurately. Considering the climate change of Inner Mongolia (Su et al., 2008; Han et al., 2010), in order to better illustrate this conclusion, we choose the data in 2005 to carry on the process of spin-up and the process of spin-up reaches a length of 10 years. We choose the time range from May, 2005 to July, 2005 as the time slot of optimization, and choose August, 2005 as the time slot of prediction in this experiment.

Table 1 and Table 2 show the numerical results of experiment Ⅰ. In Table 1 and Table 2, sand optimization refers to the optimization to sand only, clay optimization means the optimization to clay only, and sand-clay optimization refers to the optimization to sand and clay simultaneously. In order to better display the difference of the shallow soil moisture simulated by CoLM before and after optimization, we add the mean deviation as the reference function in Table 2. The mean deviation is as following:

$$f_m = \frac{\sum_{i=1}^{n} | s_i - o_i |}{n}, \qquad (10)$$

where f_m refers to the mean deviation, n represents the integral time steps, s_i is

Nonlin. Processes Geophys. Discuss., doi:10.5194/npg-2016-13, 2016
Manuscript under review for journal Nonlin. Processes Geophys.
Published: 27 January 2016

331 the simulation value at time i and o_i refers to the observation value at time i.

332 Table 1 displays the values of sand and clay before and after optimization, and
333 Table 2 shows the objective function value and the reference function value before
334 and after optimization both in the optimization slot and the prediction slot. In Table 2,
335 obj1 refers to the objective function value at the stage of optimization, obj2 refers
336 to the objective function value at the stage of prediction, ref1 refers to the reference
337 function value at the stage of optimization and ref2 refers to the reference function
338 value at the stage of prediction. It is also the case in all subsequent tables. From Table
339 2, we know that the objective function value and the reference function value are both
340 smaller after the sand optimization, the clay optimization and the sand-clay
341 optimization. In addition, it is clear that the extent of diminution is the largest after the
342 sand-clay optimization in the optimization slot. So CoLM could simulate the shallow
343 soil moisture better after each optimization and CoLM could simulate the shallow soil
344 moisture the best after the sand-clay optimization in the optimization slot. Moreover,
345 in the prediction slot, the root mean square deviation and the mean deviation are both
346 smaller after the sand optimization, the clay optimization and the sand-clay
347 optimization. And the objective function value and the reference function value are
348 both the smallest after the sand-clay optimization at the stage of prediction. That is to
349 say, CoLM could predict the shallow soil moisture better at the stage of prediction and
350 the prediction effect is the best after the sand-clay optimization.

351 To better illustrate the improvement, Figure 1 and Figure 2 are given to
352 demonstrate the numerical results of experiment Ⅰ graphically. Figure 1 shows the
353 simulations of the shallow soil moisture before and after sand optimization, the clay
354 optimization and the sand-clay optimization in the optimization slot and the prediction
355 slot. Figure 2 shows the corresponding scatter diagram of Figure 1. Here, obs stands
356 for the observation, sim1 means the simulation before the optimization, sim2
357 means the simulation after the sand optimization, sim3 means the simulation after
358 the clay optimization and sim4 means the simulation after the sand-clay
359 optimization. It is also the case in all subsequent figures.

Nonlin. Processes Geophys. Discuss., doi:10.5194/npg-2016-13, 2016
Manuscript under review for journal Nonlin. Processes Geophys.
Published: 27 January 2016

All of the above tables and figures show that, CoLM could simulate the shallow soil moisture better with the reasonable collocation of sand and clay. Sand is large and clay is relatively small before the optimization, so the soil water holding capacity is poor and the soil infiltration capacity is relatively good before the optimization. Hence it is easy for water to infiltrate into the deep soil layer and the simulation of the shallow soil moisture of CoLM before the optimization is relatively small. After sand optimization, sand becomes smaller, the soil water holding capacity is better, and the simulation of the shallow soil moisture of CoLM is larger than ever. That is to say, CoLM simulates the shallow soil moisture better after sand optimization. After the clay optimization, clay is larger and the penetrability of water is worse. So, the shallow soil moisture simulated by CoLM is larger, and the ability of simulating the shallow soil moisture of CoLM become better after the clay optimization. Sand and clay reach an appropriate combination after the sand-clay optimization, and the soil water holding capacity is better. Therefore, the simulation of the shallow soil moisture of CoLM is larger and the ability of simulating the shallow soil moisture of CoLM is better after the sand-clay optimization.

4.2 Experiment Ⅱ and the results

4.2.1 Experiment Ⅱ

In experiment Ⅱ, the forcing data and the observation data described in the section 4.1.1 are replaced by the corresponding data in dataset Ⅱ. Also, we will conduct the single-parameter optimal experiment related to sand and clay separately, and the double-parameter optimal experiment related to sand and clay simultaneously in the optimization slot. And then we will compare the simulations of CoLM with the observation data both in the optimization slot and the prediction slot.

4.2.2 The numerical results of experiment Ⅱ

Like the results of experiment Ⅰ, by a large amount of numerical experiments for many different time ranges, the numerical results show that the optimal parameters could make CoLM simulate the shallow soil moisture better. In order to illustrate this

Nonlin. Processes Geophys. Discuss., doi:10.5194/npg-2016-13, 2016
Manuscript under review for journal Nonlin. Processes Geophys.
Published: 27 January 2016

conclusion more specifically, we also choose the data in 2005 to conduct the process of spin-up and the process of spin-up reaches a length of 10 years. We still choose the time slot from May, 2005 to July, 2005 as the optimization slot and August, 2005 as the prediction slot in experiment Ⅱ.

Table 3 and Table 4 display the results of experiment Ⅱ. In these tables, sand optimization, clay optimization and sand-clay optimization mean the same as in table 1 and table 2. We also add the mean deviation as the reference function in Table 4, just like what we have done in Table 2, so that we can better exhibit the difference between the shallow soil moisture simulated by CoLM before and after optimization. From Table 4, we can see that the objective function value and the reference function value are both smaller after sand optimization, clay optimization and sand-clay optimization. Moreover, we can see that, in the optimization slot, the diminution is the largest after sand-clay optimization. This means that CoLM could simulate the shallow soil moisture better after each optimization and, after sand-clay optimization in the optimization slot, the ability to simulate the shallow soil moisture of CoLM is the best. In addition, in the prediction slot, the root mean square deviation and the mean deviation are both smaller after the sand optimization, the clay optimization and the sand-clay optimization. And the objective function value and the reference function value are both the smallest after the clay optimization at the stage of prediction. This means that CoLM could predict the shallow soil moisture better at the stage of prediction and the prediction effect is the best after the clay optimization.

In order to better illustrate the improvement, we offer Figure 3 and Figure 4 to display the numerical results of experiment Ⅱ. Figure 3 shows the simulations of the shallow soil moisture before and after sand optimization, clay optimization and sand-clay optimization at the optimization slot and the prediction slot. Figure 4 shows the corresponding scatter diagrams of Figure 3.

Table 3 and Table 4 show that CoLM could simulate the shallow soil moisture better with the reasonable proportion of sand and clay in soil. Sand is large and clay is relatively small before the optimization, so the soil water holding capacity is poor and the soil infiltration is relatively good before the optimization. Therefore water is easy

Nonlin. Processes Geophys. Discuss., doi:10.5194/npg-2016-13, 2016
Manuscript under review for journal Nonlin. Processes Geophys.
Published: 27 January 2016

418 to infiltrate into the deep soil layer and the simulation of the shallow soil moisture of
419 CoLM before the optimization is relatively small. After the sand optimization, sand is
420 smaller and hence the soil water holding capacity is better. Consequently, after the
421 sand optimization, the simulation of shallow soil moisture of CoLM is larger and
422 CoLM could simulate the shallow soil moisture better. After the clay optimization,
423 clay is larger and therefore the penetrating quality of water is worse. For this reason,
424 the shallow soil moisture simulated by CoLM is larger and the ability of simulating
425 the shallow soil moisture of CoLM is better after the clay optimization. After the
426 sand-clay optimization, sand and clay reach an appropriate combination and so the
427 soil water holding capacity is better. Hence the simulation of the shallow soil moisture
428 of CoLM is larger and the ability to simulate the shallow soil moisture of CoLM is
429 better after the sand-clay optimization. All the results of experiments (I and II) are
430 similar to Wang and Huo (2013), except that, for the NMC Reanalysis 6-hourly
431 surface fluxes data, at the stage of prediction, the cost function are much smaller than
432 those in Wang and Huo (2013).

433 Now let's focus on the peak about the shallow soil moisture in experiments (Ⅰ and
434 Ⅱ). For this case, we show the convective precipitation and large scale precipitation
435 in Figure 5. Comparing the precipitation with the shallow soil moisture simulated at
436 the stage of optimization and the stage of prediction, we find that the precipitation is
437 almost in accord with the occurrence of the peak, which means the simulations of the
438 shallow soil moisture are rational.

439 **4.3 Experiment Ⅲ and the results**

440 **4.3.1 Experiment Ⅲ**

441 Latent heat flux, as an important component of Earth's surface energy budget, is the
442 flux of heat from the Earth's surface to the atmosphere that is associated with
443 evaporation of water at the surface and subsequent condensation of water vapor in the
444 troposphere. It is very common to measure latent heat flux with the Bowen ratio
445 technique, or by eddy covariance.

446 For testing the ability of CoLM to simulate the latent heat flux, in this experiment,

Nonlin. Processes Geophys. Discuss., doi:10.5194/npg-2016-13, 2016
Manuscript under review for journal Nonlin. Processes Geophys.
Published: 27 January 2016

447 the shallow soil moisture and the latent heat flux are both chosen as the objective
448 variables. We choose the weighted root mean square deviation as the objective
449 function with the following form:

450 $$f_1 = w_1 \cdot f_r(\theta_1) + w_2 \cdot f_r(\theta_2), \quad (11)$$

451 where f_1 is the weighted root mean square deviation; θ_1 means the shallow soil
452 moisture, θ_2 is the latent heat flux; w_1 and w_2, the weight coefficients, satisfy the
453 condition: $w_1 + w_2 = 1$, and their values are decided based on the dimensions of the
454 shallow soil moisture and the latent heat flux; $f_r(\theta_1)$ and $f_r(\theta_2)$ represent the root
455 mean square deviations corresponding to the shallow soil moisture and the latent heat
456 flux respectively as formulated by Eq. (9).

457 In this experiment, we use both dataset Ⅰ and dataset Ⅱ to optimize the same
458 parameters as experiments Ⅰ and Ⅱ in the time slot of optimization. And we predict
459 the shallow soil moisture and the latent heat flux in the time slot of prediction.

460 **4.3.2 The numerical results of experiment Ⅲ**

461 The numerical results of experiment Ⅲ are given in Tables 5-8. Table 5 and Table 6
462 show the results with dataset Ⅰ, and Table 7 and Table 8 with dataset Ⅱ. We add the
463 reference function of weighted mean deviation in Table 5 and Table 7 to better display
464 the variation of the shallow soil moisture before and after optimization. The reference
465 function of weighted mean deviation refers to the following relation:

466 $$f_2 = w_1 \cdot f_m(\theta_1) + w_2 \cdot f_m(\theta_2), \quad (12)$$

467 where f_2 means the weighted mean deviation; θ_1 is the shallow soil moisture; θ_2
468 is the latent heat flux; the weight coefficients, w_1 and w_2, satisfy the condition:
469 $w_1 + w_2 = 1$, and their values are chosen based on the dimensions of the shallow soil
470 moisture and the latent heat flux; $f_m(\theta_1)$ represents the mean deviation corresponding
471 to the shallow soil moisture formulated by Eq. (10); $f_m(\theta_2)$ means the mean
472 deviation corresponding to the latent heat flux formulated by Eq. (10).

473 Table 5 and Table 7 show the objective function values and reference function
474 values before and after parameter optimization. Table 6 and Table 8 show the
475 percentage of sand and the percentage of clay in soil before and after parameter

Nonlin. Processes Geophys. Discuss., doi:10.5194/npg-2016-13, 2016
Manuscript under review for journal Nonlin. Processes Geophys.
Published: 27 January 2016

optimization. The results are consistent with the results in experiment Ⅰ and experiment Ⅱ.

From what we have discussed above, the extended application of CNOP-P method in CoLM is reasonable and efficient.

5. Discussions and Conclusions

From the above three experiments, we can see that the optimized parameters after sand optimization, clay optimization and sand-clay optimization could make CoLM simulate the objective variable(s) better at the stage of optimization, and it is the best after sand-clay optimization. Moreover, the optimized parameters could enable CoLM to improve its ability of simulation observably at the stage of prediction in these three experiments. The difference of the numerical results between experiment Ⅰ and experiment Ⅱ is that, at the stage of prediction, the optimal parameters after the sand-clay optimization attained in experiment Ⅰ could make CoLM simulate the shallow soil moisture the best, which is rational, but in experiment Ⅱ, the optimal parameters attained by clay optimization could make the ability of simulating the shallow soil moisture of CoLM the best, which is not line with the common sense.

These conclusions are similar to Wang and Huo (2013), although the climate of the research areas is different, one is a arid and semiarid area, and the other is subhumid temperate climate. At the same time, dataset Ⅰ are the revise of dataset Ⅱ, and dataset Ⅰ are more accurate than dataset Ⅱ. As we all know, the simulating ability of CoLM depends on the accuracy of data, such as forcing data, initial data, boundary data and so on, and in general, the more accurate the data are, the more reliable the simulations will be. In our works, we got similar results for both arid and semiarid and subhumid area, so, we can guess that the factor affecting optimal results and simulating ability mainly is the accuracy of dataset. The more accurate the dataset are, the more trustworthy the optimal results will be.

The conclusions obtained in this work also show that the extended application of CNOP-P method in CoLM is reasonable and efficient. But we just investigated two special parameters and in one special area, i.e. the Hulunbiur Steppe. It will be

Nonlin. Processes Geophys. Discuss., doi:10.5194/npg-2016-13, 2016
Manuscript under review for journal Nonlin. Processes Geophys.
Published: 27 January 2016

505 beneficial and helping to lay solid foundations for ecosystem management to consider
506 more important parameters in CoLM in arid and semiarid areas.
507

Nonlin. Processes Geophys. Discuss., doi:10.5194/npg-2016-13, 2016
Manuscript under review for journal Nonlin. Processes Geophys.
Published: 27 January 2016

Nonlinear Processes in Geophysics
Discussions
Open Access
EGU

508 **Author contribution**

509 Bo Wang designed the experiments and wrote up the manuscript with contributions
510 from all co-authors, Zhenhua Huo carried the experiments out, and Yujing Yuan and
511 Shang Wu helped to check the model code and the simulations.

512

Nonlin. Processes Geophys. Discuss., doi:10.5194/npg-2016-13, 2016
Manuscript under review for journal Nonlin. Processes Geophys.
Published: 27 January 2016

Nonlinear Processes in Geophysics
Discussions
Open Access
EGU

Acknowledgements

This research was supported by the National Natural Science Foundation of China (Grant No. 40805020); the Open Subject of LASG, IAP, CAS(No. 201401); the foundation for Young University Key Teacher by the Educational Department of Henan Province (No. 2014GGJS-021); the Emerging Cross and Characteristic Discipline Plan of Henan University(No. 0000A40450). The authors are grateful to NOAA/OAR/ESRL PSD, Boulder, Colorado, USA, for the availability of the NCEP Reanalysis and NCEP_Reanalysis 2 data from their website (http://www.esrl.noaa.gov/psd).

Nonlin. Processes Geophys. Discuss., doi:10.5194/npg-2016-13, 2016
Manuscript under review for journal Nonlin. Processes Geophys.
Published: 27 January 2016

References

Bastidas, L. A., Hogue, T. S., Sorooshian, S., Gupta, H.V., and Shuttleworth, W. J.: Parameter sensitivity analysis for different complexity land surface models using multicriteria methods, J. Geophys. Res., 111, 2006, doi: 10.1029/2005JD006377.

Bonan, G. B.: A land surface model (LSM version 1.0) for ecological, hydrological, and atmospheric studies: Technical description and user's guide. NCAR Tech. Note NCAR/TN-417+STR, 150 pp, 1996.

Dai, Y. J. and Coauthors: Common Land Model (CLM): Technical Documen- tation and User's Guide. http://globalchange.bnu.edu.cn/research/models, 2001.

Dai, Y. J. and Zeng Q.-C.: A land surface model (IAP94) for climate studies, Part I: Formulation and validation in off-line experiments. Adv. Atmos. Sci., 14, 433–460, 1997.

Dickinson, R. E., Henderson-Sellers, A., Kennedy, P. J., and Wilson, M. F.: Biosphere–Atmosphere Transfer Scheme (BATS) version 1e as coupled to Community Climate Model. NCAR Tech. Note NCAR/TN-387+STR, 72 pp, 1993.

Duan, W. S., Mu, M. and Wang, B.: Conditional nonlinear optimal perturbations as the optimal precursors for El Nino–Southern Oscillation events. J. Geophys. Res., 109, D23105, 2004.

Duan, W. S. and Mu, M.: Investigating decadal variability of El Nino–Southern Oscillation asymmetry by conditional non-linear optimal perturbation. J. Geophys. Res., 111, C07015, 2006.

Duan, W. S., Xu, H. and Mu, M.: Decisive role of nonlinear temperature advection in El Nino and La Nina amplitude asymmetry. J. Geophys. Res., 113, C01014, 2008.

Duan, W. S. and Mu, M.: Conditional nonlinear optimal perturbation: applications to stability, sensitivity, and predictability. Science in China (D) : Earth Sciences, 52, 7, 883-906, 2009.

Duan, W. S., Xue, F. and Mu, M.: Investigating a nonlinear characteristic of ENSO events by conditional nonlinear optimal perturbation. Atmos. Res., 94, 10-18, 2009a.

551 Duan, W. S., Liu, X. C., Zhu, K. Y. and Mu, M.: Exploring the initial error that causes
552 a significant spring predictability barrier for El Nino events. J. Geophys. Res., 114,
553 C04022, 2009b.
554 Duan, W. S. and Luo, H. Y.: A new strategy for solving a class of nonlinear
555 optimization problems related to weather and climate predictability. Adv. Atmos. Sci.,
556 4, 741-749, 2010.
557 Duan, W. S. and Zhang, R.: Is model parameter error related to spring predictability
558 barrier for El Nino events? Adv. Atmos. Sci., 5, 1003–1013, 2010.
559 Han, F., Niu, J. M., Liu, P. T., Na, R. S. , Zhang Y. N., Wan G. H.: Impact of Climate
560 Change on Forage Potential Climatic Productivity in Desert Steppe in Inner Mongolia.
561 Chin. J. Grassl., 32(5), 57-65, 2010. (in Chinese)
562 He, Y. C. and Wang, X. Z.: Solution of Hard Constrained Optimization Problem
563 Based on Modified Differential Evolution Algorithm. Comput. Eng., 34, 193-217,
564 2008. (in Chinese)
565 Li, H. Q., Guo, W. D., Sun, G. D. and Zhang, Y. C.: Using conditional nonlinear
566 optimal perturbation method in parameter optimization of land surface processes
567 model. Acta. Phys. Sin., 60, 019201, 1-7, 2011a. (in Chinese)
568 Li, H. Q., Guo, W. D., Sun, G. D., Zhang, Y. C. and Fu, C.B.: A new approach for
569 parameter optimization in land surface model. Adv. Atmos. Sci., 28(5), 1056-1066,
570 doi: 10.1007/s00376-010-0050-z, 2011b.
571 Liu, B., Wang, L., and Jin, Y. H.: Advances in differential evolution. Control. Decis.,
572 22, 721-729, 2007. (in Chinese)
573 Luo, S. Q., Lu, S. H., Zhang, Y., Hu, Z. Y., Ma, Y. M., Li, S. S. and Shang, L. Y.:
574 Simulation Analysis on Land Surface Process of BJ Site of Central Tibetan Plateau
575 Using CoLM. Plateau Meteor., 27, 259-271, 2008. (in Chinese)
576 Ma, Q. Y.. It's hot and sunny in the eastern part in late May and frequently rainy with
577 sleet in the southern part. Meteor. Mon., 18(8), 62-63, 1992. (in Chinese)
578 Meng, C. L. and Cui, J. Y.: Study on Soil Evaporation and Coupling Transmission of
579 Soil Moisture and Heat in Arid Areas. Arid Zone Res., 24, 141-145, 2007. (in
580 Chinese)

Nonlin. Processes Geophys. Discuss., doi:10.5194/npg-2016-13, 2016
Manuscript under review for journal Nonlin. Processes Geophys.
Published: 27 January 2016

Mu, M., and Duan, W. S.: A new approach to studying ENSO predictability: conditional nonlinear optimal perturbation. Chinese Sci. Bull., 48, 1045-1047, 2003.

Mu, M., Duan, W. S., and Wang, B.: Conditional nonlinear optimal perturbation and its applications. Nonlin. Processes Geophys., 10, 493-501, 2003.

Mu, M. and Wang, B.: Nonlinear instability and sensitivity of a theoretical grassland ecosystem to finite-amplitude perturbations. Nonlin. Processes Geophys., 14, 409–423, 2007.

Mu, M., Duan, W. S., Wang, Q., and Zhang, R.: An extension of conditional nonlinear optimal perturbation approach and its applications. Nonlin. Processes Geophys., 17, 211-220, 2010.

Song, Y. M., Guo, W. D., and Zhang, Y. C.: Performances of CoLM and NCAR_CLM3.0 in simulating land-atmosphere interactions over typical forest ecosystem in China. Part Ⅰ: Preliminary analysis of the simulations based on different models. Climatic Environ. Res., 14, 229-242, 2009a. (in Chinese)

Song, Y. M., Guo, W. D., and Zhang, Y. C.: Performances of CoLM and NCAR_CLM3.0 in simulating land-atmosphere interactions over typical forest ecosystem in China. Part Ⅱ: Impact of different parameterization schemes on simulations. Climatic Environ. Res., 14, 243-257, 2009b. (in Chinese)

Storn, R. and Price K.: Differential Evolution - A simple and Efficient Adaptive Scheme for Global Optimization Over Continuous Spaces. ICSI Technical Report TR-95-012, 12 pp, 1995.

Su, L. J., Li, X. C. and Deng, X. D.: Climate change characteristics of Eastern Inner Mongolia from 1951-2005. J. Meteor. Environ., 24(5), 2008. (in Chinese)

Sun, S. F.. Biophysical and Biochemical Mechanisms and Their Parameterization in Context of Land Surface Processes. China Meteorological Press, Beijing, 307pp, 2005. (in Chinese)

Sun, G. D. and Mu M.: A preliminary application of the differential evolution algorithm to calculate the CNOP. Atmos. Oceanic Sci. Lett., 2, 381-385, 2009.

Sun, G. D. and Mu M.: Response of a Grassland Ecosystem to Climate Change in a Theoretical Model. Adv. Atmos. Sci., 28, 1266-1278, 2011.

611 Sun, G. D. and Mu M.: Understanding variations and seasonal characteristics of net
612 primary production under two types of climate change scenarios in China using the
613 LPJ model. Climatic Change, 120, 755-769, 2013.
614 Sun, G. D. and Mu M.: The analyses of the net primary production due to regional and
615 seasonal temperature differences in eastern China using the LPJ model. Ecol. Model.,
616 289, 66-76, 2014.
617 Wang, B., Wang, J. P., Huo, Z. H., Zhang, P. J., and Wang Q.: Application of
618 Conditional Nonlinear Optimal Perturbation Method in a Theoretical Grassland
619 Ecosystem. Chinese Q. J. Math., 25, 3, 422-429, 2010.
620 Wang, B., Zhang, P. J., Huo, Z. H., and Qi, Q. Q.: The sensitivity analysis of a lake
621 ecosystem with the conditional nonlinear optimal perturbation method, Adv.
622 Meteorol., Article ID 562081, 7pages, 2012.
623 Wang, B. and Huo, Z. H.: The extended application of the conditional nonlinear
624 optimal parameter perturbation method in Common Land Model. Adv. Atmos. Sci.,
625 30(4), 1213–1223, 2013.
626 Xia, Y. L., Pitman, A. J., Gupta, H. V., Lepastrier, M., Henderson-Sellers, A., and
627 Bastidas, L. A.: Calibrating a land surface model of varying complexity using
628 multi-criteria methods and the Cabauw data set. J. Hydrometeorol., 3, 181-194, 2002.
629 Xia, Y. L., Sen, M. K., Jackson, C. S. and Stoffa, P. L.: Multi-dataset study of optimal
630 parameter and uncertainty estimation of a land surface model with Bayesian stochastic
631 inversion and Multicriteria method. J. Appl. Meteor., 43, 1477-1497, 2004a.
632 Xia, Y. L., Yang, Z. L., Jackson, C., Stoffa, P. L., and Sen, M. K.: Impacts of data
633 length on optimal parameter and uncertainty estimation of a land surface model. J.
634 Geophys. Res., 109, doi: 10.1029/2003JD004419, 2004b.
635 Xin, Y. F., Bian, L. G., and Zhang, X. H.: The Application of CoLM to Arid Region of
636 Northwest China and Qinghai-Xizang Plateau. Plateau Meteorol., 25, 567-574, 2006.
637 (in Chinese)
638 Yu, G. Y., Li, P., He, Z., and Sun, Y. M.: Advanced evolutionary algorithm used in
639 multi-objective constrained optimization problem. Comp. Integ. Manufact. Sys., 15,
640 1172-1178, 2009. (in Chinese)

Nonlin. Processes Geophys. Discuss., doi:10.5194/npg-2016-13, 2016
Manuscript under review for journal Nonlin. Processes Geophys.
Published: 27 January 2016

641 Zhang, C., Gao, J., Zhao, Y. l.: Climate changes analysis in the Inner Mongolia desert
642 grassland based on GIS. Pratacultur. Sci., 2014, 31(12): 2212-2220.(in Chinese)
643 Zheng, J., Xie, Z. H., Dai, Y. J., Yuan, X., and Bi, X. Q.: Coupling of the common
644 land model (CoLM) with the regional climate model (RegCM3) and its preliminary
645 validation. Chin. J. Atmos. Sci., 33, 737-750, 2009. (in Chinese)

Nonlin. Processes Geophys. Discuss., doi:10.5194/npg-2016-13, 2016
Manuscript under review for journal Nonlin. Processes Geophys.
Published: 27 January 2016

Nonlinear Processes in Geophysics
Discussions
Open Access
EGU

646 **Figure captions**

647 FIG.1 Sequence diagram of the shallow soil moisture (unit: m^3m^{-3}) in the experiment
648 Ⅰ. (a): at the stage of optimization; (b): at the stage of prediction.
649
650 FIG.2 Scatter diagram of the shallow soil moisture (unit: m^3m^{-3}) in the experiment Ⅰ.
651 (a): at the stage of optimization; (b): at the stage of prediction.
652
653 FIG.3 Sequence diagram of the shallow soil moisture (unit: m^3m^{-3}) in the experiment
654 Ⅱ. (a): at the stage of optimization; (b): at the stage of prediction.
655
656 FIG.4 Scatter diagram of the shallow soil moisture (unit: m^3m^{-3}) in the experiment Ⅱ.
657 (a): at the stage of optimization; (b): at the stage of prediction.
658
659 FIG.5 Convective precipitation and large scale precipitation in experiment Ⅰ and
660 experiment Ⅱ. (a): at the stage of optimization in the experiment Ⅰ; (b): at the stage
661 of prediction in the experiment Ⅰ; (c): at the stage of optimization in the experiment
662 Ⅱ; (d): at the stage of prediction in the experiment Ⅱ.

Nonlin. Processes Geophys. Discuss., doi:10.5194/npg-2016-13, 2016
Manuscript under review for journal Nonlin. Processes Geophys.
Published: 27 January 2016

Nonlinear Processes in Geophysics
Discussions
Open Access
EGU

663

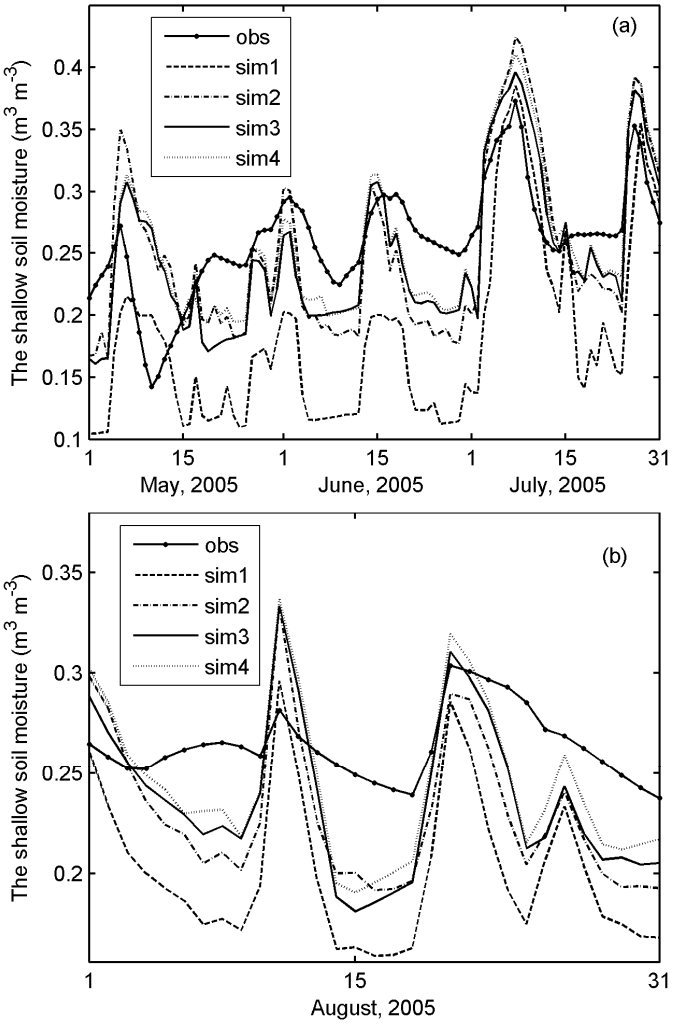

664

665

666 Fig. 1

Nonlin. Processes Geophys. Discuss., doi:10.5194/npg-2016-13, 2016
Manuscript under review for journal Nonlin. Processes Geophys.
Published: 27 January 2016

Nonlinear Processes in Geophysics
Discussions
Open Access
EGU

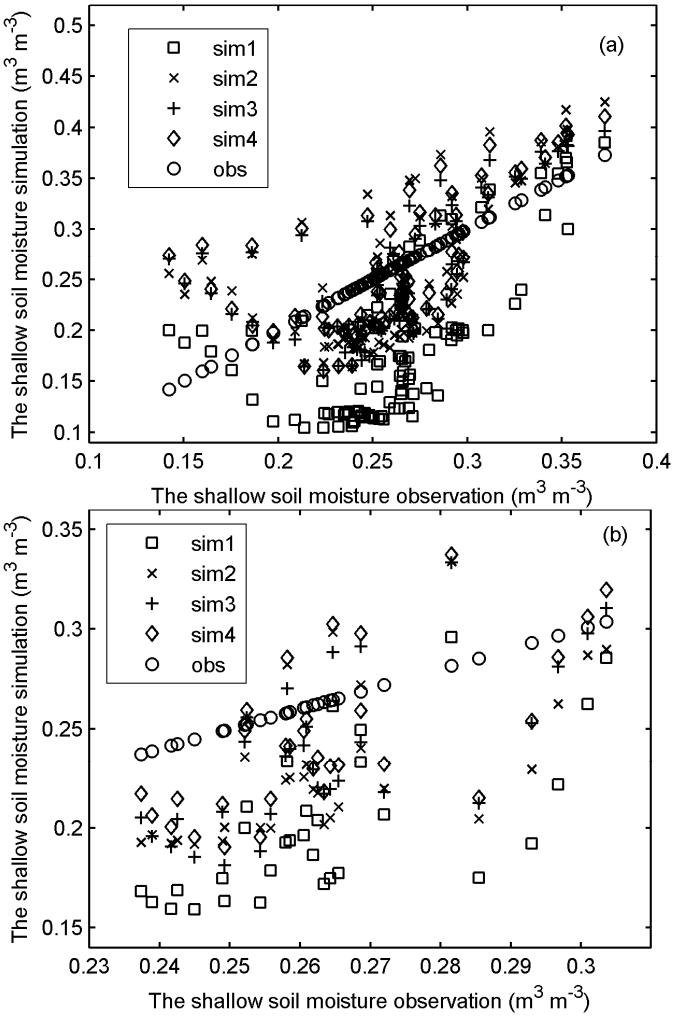

Fig. 2

Nonlin. Processes Geophys. Discuss., doi:10.5194/npg-2016-13, 2016
Manuscript under review for journal Nonlin. Processes Geophys.
Published: 27 January 2016

Nonlinear Processes in Geophysics
Discussions
Open Access
EGU

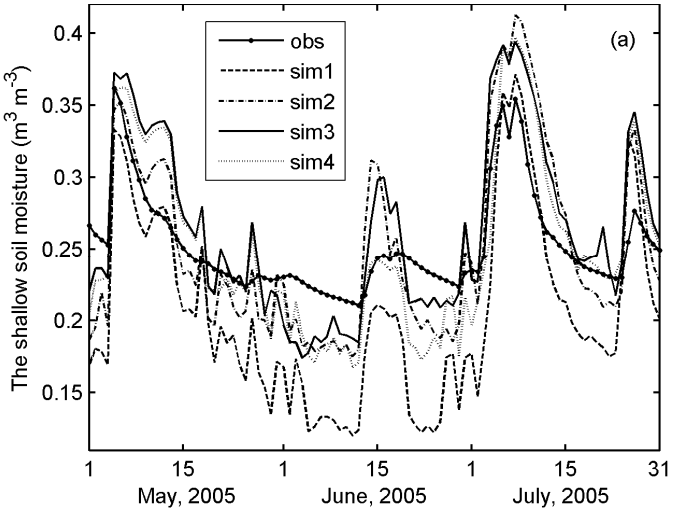

670

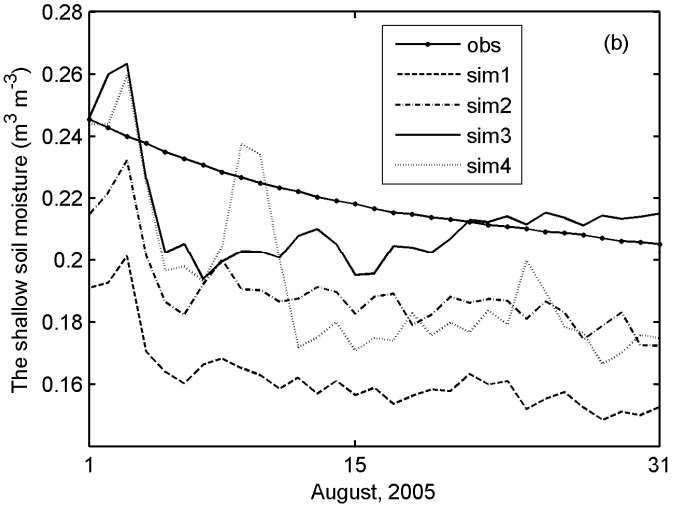

671

672 Fig. 3

Nonlin. Processes Geophys. Discuss., doi:10.5194/npg-2016-13, 2016
Manuscript under review for journal Nonlin. Processes Geophys.
Published: 27 January 2016

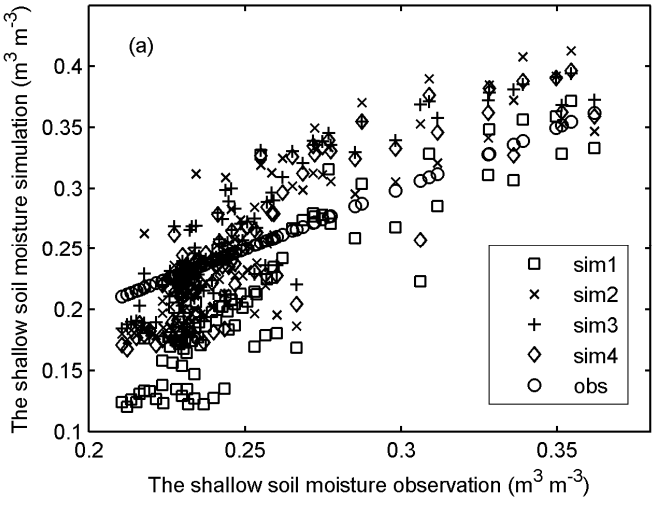

673

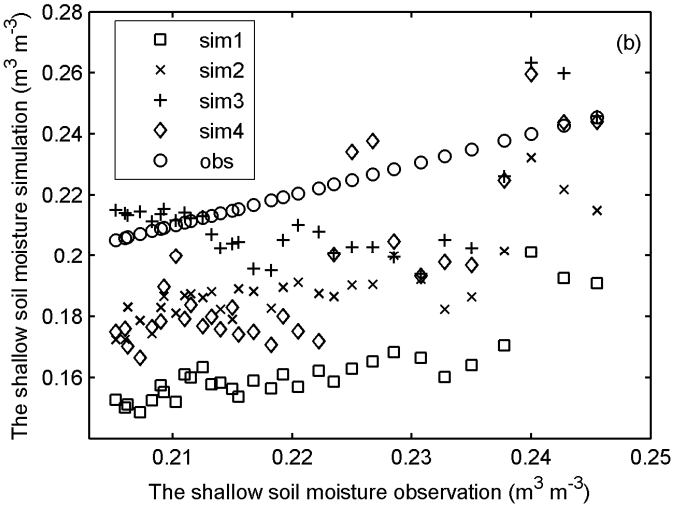

674

675 Fig. 4

676

Nonlin. Processes Geophys. Discuss., doi:10.5194/npg-2016-13, 2016
Manuscript under review for journal Nonlin. Processes Geophys.
Published: 27 January 2016

Nonlinear Processes in Geophysics
Discussions
Open Access
EGU

677

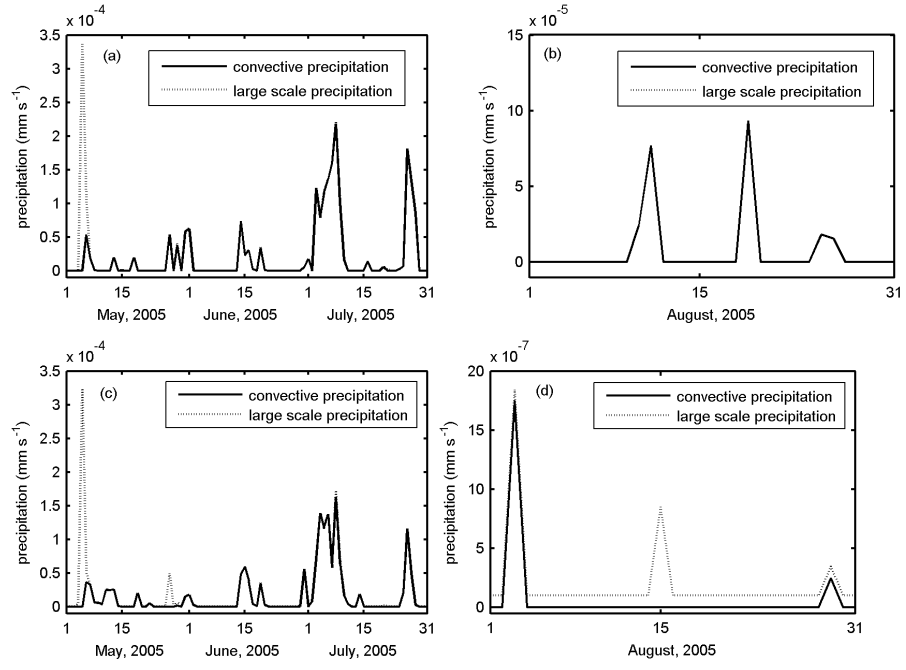

678

679 Fig. 5

Nonlin. Processes Geophys. Discuss., doi:10.5194/npg-2016-13, 2016
Manuscript under review for journal Nonlin. Processes Geophys.
Published: 27 January 2016

Nonlinear Processes in Geophysics
Discussions
Open Access
EGU

680 **Table captions**

681 Table 1. Comparison of sand and clay (unit: %) before and after optimization in the
682 experiment Ⅰ.

683

684 Table 2. Comparison of the objective function values and the referential function
685 values before and after optimization in the experiment Ⅰ.

686

687 Table 3. Comparison of sand and clay (unit: %) before and after optimization in the
688 experiment Ⅱ.

689

690 Table 4. Comparison of the objective function values and the referential function
691 values before and after optimization in the experiment Ⅱ.

692

693 Table 5. Comparison of the objective function values and the referential function
694 values before and after optimization with dataset Ⅰ in the experiment Ⅲ.

695

696 Table 6. Comparison of sand and clay (unit: %) before and after optimization with
697 dataset Ⅰ in the experiment Ⅲ.

698

699 Table 7. Comparison of the objective function values and the referential function
700 values before and after optimization with dataset Ⅱ in the experiment Ⅱ.

701

702 Table 8. Comparison of sand and clay (unit: %) before and after optimization with
703 dataset Ⅱ in the experiment Ⅱ.

Nonlin. Processes Geophys. Discuss., doi:10.5194/npg-2016-13, 2016
Manuscript under review for journal Nonlin. Processes Geophys.
Published: 27 January 2016

Nonlinear Processes in Geophysics
Discussions
Open Access
EGU

704

705 Table 1.

The parameter	Before the optimization	After sand optimization	After clay optimization	After sand-clay optimization
Sand	37.5	15.458379	37.5	28.841991
Clay	26	26	43.715421	40.281376

706

707 Table 2.

Function value	Before the optimization	After sand optimization	After clay optimization	After sand-clay optimization
obj1	0.098224	0.056424	0.050492	0.049054
ref1	0.087392	0.050470	0.043871	0.042262
obj2	0.069606	0.045452	0.040497	0.036333
ref2	0.063743	0.041387	0.035004	0.031494

708

709 Table 3.

The parameter	Before the optimization	After sand optimization	After clay optimization	After sand-clay optimization
Sand	37.5	11.215094	37.5	42.190752
Clay	26	26	52.195857	54.614659

710

711 Table 4.

Function value	Before the optimization	After sand optimization	After clay optimization	After sand-clay optimization
obj1	0.061491	0.038930	0.036811	0.036528
ref1	0.053017	0.032882	0.030984	0.029458
obj2	0.058472	0.032212	0.017816	0.033081
ref2	0.057880	0.030818	0.014367	0.030414

Nonlin. Processes Geophys. Discuss., doi:10.5194/npg-2016-13, 2016
Manuscript under review for journal Nonlin. Processes Geophys.
Published: 27 January 2016

712 Table 5.

Function value	Before the optimization	After sand optimization	After clay optimization	After sand-clay optimization
obj1	0.190404	0.135727	0.131815	0.128480
ref1	0.138981	0.107459	0.105064	0.099933
obj2	0.135303	0.104008	0.086822	0.083889
ref2	0.117531	0.083503	0.065347	0.062849

713

714 Table 6.

The parameter	Before the optimization	After sand optimization	After clay optimization	After sand-clay optimization
Sand	37.5	11.227582	37.5	37.489331
Clay	26	26	46.279844	46.089471

715

716 Table 7.

Function value	Before the optimization	After sand optimization	After clay optimization	After sand-clay optimization
obj1	0.214117	0.156524	0.152562	0.146493
ref1	0.169689	0.119458	0.115074	0.110053
obj2	0.172814	0.150163	0.154181	0.143004
ref2	0.141641	0.117755	0.122391	0.111130

717

718 Table 8.

The parameter	Before the optimization	After sand optimization	After clay optimization	After sand-clay optimization
Sand	37.5	11.860160	37.5	25.993371
Clay	26	26	36.664604	40.290898

719